Yang et al. Journal of Wood Science (2022) 68:50
https://doi.org/10.1186/s10086-022-02051-4

Journal of Wood Science

ORIGINAL ARTICLE Open Access

Research on the wood processing method of helium-assisted laser process

Chunmei Yang[1], Xinchi Tian[1], Bo Xue[1], Qingwei Liu[1], Jiawei Zhang[1], Jiuqing Liu[1] and Wenji Yu[1,2*]

Abstract

In order to promote the development of environmental protection, and the usage rate of green energy utilization, a progressive, innovative laser process method employing helium assisted is proposed, which optimizes the joint cutting process under the same energy consumption. This method provides a new idea for the wood process industry. The uniqueness of this paper establishes a mathematical model to address the diffusion of helium injection and the heat transfer of the laser beam on the processed surface. From the results, it can be exhibited that the oxygen concentration reduces when the helium is injected on the processed surface. The helium could destroy the combustion-supporting conditions and decrease the combustion zone of the processed joint cutting. Thus, the carbonized area of the processed surface is reduced, which could effectively enhance the processing quality of joint cutting. Notably, the helium with injection speed forms a sweeping effect on the processed surface, which could remove parts of the carbonized particles and residues on the processed surface, as well as improve the processing quality. Comparing the traditional laser process and helium-assisted laser process, the gas-assisted laser process owns higher process quality than that of traditional laser processing and cutting. In detail, it features the advantages of smaller joint cutting width, lower surface roughness and smoother surface. Eventually, a mathematical model based on the response surface method with the evaluation criteria of the kerf width, kerf depth, and surface roughness is established to analyze the interaction of laser power, cutting speed and inert gas pressure on the response factors. Comparing the error between the predicted and experimental measurement value, and the optimized process parameters could be acquired. In this paper, the helium-assisted laser process method proposed is meaningful and encouraging, which not only obtains better processing quality, but also provides a guide for developing green industry.

Keywords: Helium assisted, Laser processing, Heat transfer model, Response surface method

Introduction

With the change of world climate and the enhancement of people's awareness of environmental protection, reducing pollution, improving air quality and forest coverage have become major issues all over the world. As for the primary component of forests, wood plays an indispensable role in the national economy. Compared with other materials, such as metal, wood has the advantages of high specific strength, impact resistance, facile processing and renewable resources. These features have been widely employed in the fields of housing construction, paper industry, home decoration, road construction and energy application [1]. Additionally, wood products are irreplaceable to a certain extent. At present, the comprehensive utilization rate of wood in China is about 63%, while that in Australia and other world forestry developed countries has reached more than 80% [2]. The traditional wood processing primarily includes milling, sawing and polishing. The main problems of these methods are the wide sawing path, large machining allowance, inability to process at any positions and difficulty in processing complex wood products. Therefore, the utilization rate of wood cannot be thoroughly improved [3]. Affected by the mechanical properties, geometry, machining tool

*Correspondence: chinayuwj@126.com

[1] Northeast Forestry University, 26 Hexing Rd, Harbin 150040, China
Full list of author information is available at the end of the article

accuracy and machining methods of the processed wood, the processed products will have defects such as wood grain bulge, burr, wavy knife mark and chip indentation, affecting the machining accuracy and appearance quality of components [4]. Therefore, adopting a new processing technology and method to improve the utilization efficiency of wood and the processing quality of processed parts on the premise of equal resource consumption has important practical significance for the overall goal of resource conservation of wood and international environmental protection.

Laser processing of wood is an advanced processing technology derived from the field of metal material processing. Due to the characteristics of high laser intensity, good monochromaticity and good directivity, it is widely used in wood manufacturing industry, resulting in technologies such as rapid processing, tomography and nondestructive testing [5, 6]. Combined with computer control system and automatic equipment, laser beam profiling cutting is employed to achieve the forming processing of parts [7, 8], which could effectively make up for the tool wear, size limitation, complex contour of parts in traditional cutting methods. The influence of self-stability and other constraints on the machining process, especially for thin plates and small-size parts, has better flexibility and adaptability [9, 10]. However, in the traditional laser processing process, as the laser beam temperature is generally between 1200 ℃ and 1500 ℃, it registers ultra-high temperature and energy. Under the thermal coupling between the laser beam and the material, the commensurately laser beam would produce severe ablation on the surface of wood, and then form a wide carbonization layer on the processing surface, which seriously affects the processing accuracy and quality. Therefore, a method is sought to reduce the ablation effects in laser processing and recline the width of carbonization layer, so as to enhance the machining accuracy and quality of the workpiece.

Our team has put forward the process method of water jet-assisted laser processing wood, and conducted a large number of relevant research and experiments. The synergistic and cooling effect of water jet has tremendously improved the width and surface roughness of wood [11–13], but the refraction phenomenon would occur in the process of laser penetrating water jet, resulting in laser energy loss. Meanwhile, the water jet sprayed on the machined surface would have an abundant impact on the moisture content of wood, and increase the instability of the processed material. Focusing on the technical problems of large ablation range, viz. low machining accuracy and poor machining quality in laser machining, this paper proposes an advanced process method of laser machining assisted by inert gas, which is more suitable for laser processing. Laser and inert gas are sprayed from the nozzle at the same time to cut wood at a height of 1–2 mm from the processing plane. The inert gas could effectively reduce the oxygen concentration of the processed surface, and destroy the combustion-supporting conditions of ablation, which reduces the ablation area of the processed surface. This method could effectively reduce the ablation and carbonization range of the processed surface, and then enhance the processing quality, providing a reference for the popularization and application of wood material in laser processing technology. The feasibility of the process by means of theoretical modeling and experimental has been conducted objectively. Notably, it is of great significance to improve the process level and production efficiency in wood processing industry. In the meantime, it also has practical significance for the economical utilization of wood resources and the protection of global ecological environment.

Model

When the laser cooperates with the inert gas emitted from the coaxial nozzle, the initial velocity of the gas is about 10 m/s. The emitted gas absorbs energy in the space and forms turbulence. Meanwhile, the gas is also diffused by the gas flow and the concentration decreases along the direction perpendicular to the axis. As the cutting quality of the machined part is caused by high-temperature ablation, it is vital to employ the mathematical model to solve the ablation area on the machined surface. The gas jet flow during laser cutting is shown in Fig. 1.

Establishment of model

The three elements of combustion are combustibles, combustion-supporting gas and ignition point. When the laser is processed under the helium package, the scattering degree of the laser would further affect the generation and transfer of heat. In the meantime, the helium would diffuse at a certain initial velocity after being sprayed from the nozzle, so the gas concentration would also be reduced in the plane perpendicular to the nozzle.

In the mixture of helium and oxygen, when the oxygen content is higher than 12.5%, wood can burn, and when it is lower than 12.5%, it is not combustible. Therefore, it is crucial to calculate the proportion of oxygen at any points. The oxygen content is also affected by the diffusion of helium. Therefore, it is critical to calculate the helium concentration at each point. Meanwhile, whether the processed surface burns also depends on the amount of heat transmitted through the wood. The ignition point of the wood is generally

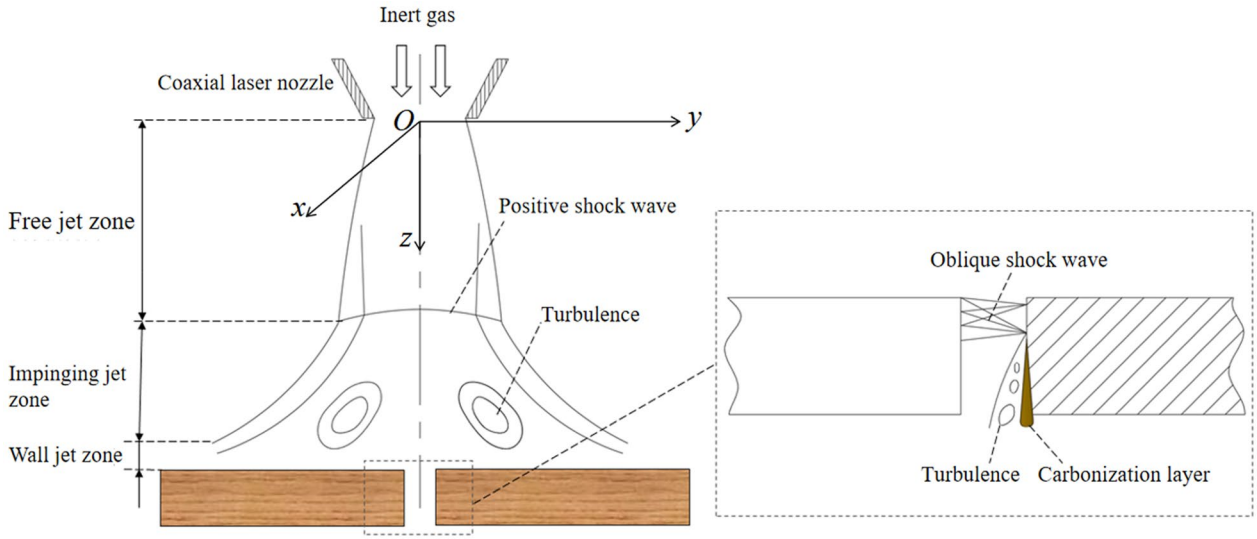

Fig. 1 Gas-assisted jet partition in the cutting process

between 200 and 300 ℃. The ignition point of the original wood studied in this paper is approximately 280 ℃. Comprehensively, whether the machined surface burns or not is determined by the oxygen concentration and surface temperature.

Basic assumptions

In order to simplify the mathematical model and solution process, the following assumptions are put forward:

(1) The material is anisotropic in the heat diffusion direction, namely, the heat diffusion rate at each point remains constant but is randomly distributed among each other.
(2) The mass of inert gas is conserved in the diffusion process. The gas concentration in the diffusion process obeys the normal distribution in the y and z directions, and the flow rate does not exceed 68 m/s, which is regarded as an incompressible fluid.
(3) In the process of laser spraying, each point on the laser beam is supposed to be isothermal, regardless of the temperature drop caused by the emission distance.
(4) The indoor gas flow is stable and the helium concentration does not change with time.
(5) As the laser source is only 1 mm relative to the processing distance, the blocking effect of wood thickness processed by steam plasma on laser is ignored.
(6) Ignore the combustion effects of small sawdust produced by processing.

Gas diffusion model

Taking the injection point as the origin and the injection direction as the z-axis direction, a spatial rectangular coordinate is established. The effective point source is located at the coordinate origin o, and the average velocity direction is parallel to and in the same direction as the z-axis. The Reynolds number of helium jet flow is higher than the critical value and flows as turbulent flow. When the jet stream ejects the inert gas from the nozzle at the velocity v_0, the surrounding fluid is continuously pumped in the flow, the width of the jet is expanded, and the velocity of the main body of the gas is constantly reduced. The jet diffusion angle is θ. According to the momentum theorem, the momentum along the jet velocity direction remains unchanged at any interface of the jet, so it can be obtained:

$$\int \rho v^2 dA = \rho_0 v_0^2 A_0 = \rho_0 \pi R_0^2 v_0^2 = 2\pi \int_0^R \rho v^2 r dr. \quad (1)$$

In the above formula, A_0 is the cross-sectional area at the nozzle, R_0 is the nozzle radius and the helium density at the nozzle is ρ_0. Since the jet density is the same as that of the surrounding air, that is $\rho = \rho_0$, formula (1) can be rewritten as:

$$2\int_0^{\frac{R}{R_0}} \left(\frac{v}{v_0}\right)^2 \frac{r}{R_0} d\left(\frac{r}{R_0}\right) = 1. \quad (2)$$

Also $\frac{r}{R_0} = \frac{r}{R} \cdot \frac{R}{R_0}$, $\frac{R}{R_0}$ determined by the distance from any cross section to the jet pole. Therefore, $\frac{v}{v_0} = \frac{v}{v_m} \cdot \frac{v_m}{v_0}$. So Eq. (2) can be exhibited as:

$$2\left(\frac{v_m}{v_0}\right)^2\left(\frac{R}{R_0}\right)^2\int_0^1\left(\frac{v}{v_m}\right)^2\frac{r}{R}d\left(\frac{r}{R}\right)=1. \tag{3}$$

Herein, v_m is the velocity on the axis of inert gas injection. In terms of the above formula, the inert gas flow on any section is:

$$\begin{aligned} q &= 2\pi\int_0^R vrdr = 2\pi R_0^2 v_0\left(\frac{R}{R_0}\right)^2\frac{v_m}{v_0}\int_0^1\frac{v}{v_m}\frac{r}{R}d\left(\frac{r}{R}\right)\\ &= 2q_0\left(\frac{R}{R_0}\right)^2\frac{v_m}{v_0}\int_0^1\left[1-\left(\frac{r}{R}\right)^{\frac{3}{2}}\right]^2\frac{r}{R}d\left(\frac{r}{R}\right). \end{aligned} \tag{4}$$

Among them, q_0 the inert gas flow initially ejected from the nozzle can be calculated at any point according to Eq. (4).

The concentration change of inert gas in the atmosphere is jointly determined by jet and diffusion. As for the gas diffusion, we adopt the steady Gaussian diffusion model. The point source is located at the coordinate origin, so its diffusion can be regarded as gas diffusion at height 0. The diffusion in air is a two-dimensional normal distribution with two coordinate directions of y and z. When the random variables in the two coordinate directions are independent, the distribution density is the product of the one-dimensional normal distribution density function in each coordinate direction. According to the assumption of Gaussian gas diffusion model, taking $\mu=0$,the gas concentration distribution function at any points in the velocity direction of point source can be acquired as follows:

$$C(x,y,z)=A(x)\exp\left[-\frac{1}{2}\left(\frac{y^2}{\sigma_y^2}+\frac{z^2}{\sigma_z^2}\right)\right]. \tag{5}$$

In the above formula, C—concentration of pollutants at space point (x, y, z); $A(x)$—undetermined function; σ_y, σ_z—standard deviations in the horizontal and vertical directions, i.e., the diffusion parameters in the y and z directions, mm.

According to the law of conservation of mass and the continuity theorem, on any cross section of air flow perpendicular to the z-axis:

$$q=\int_{-\infty}^{+\infty}\int_{-\infty}^{+\infty}Cudydz. \tag{6}$$

Equation (1) is substituted into Eq. (2) by the velocity stability condition, a is independent of x and y, and $\int_{-\infty}^{+\infty}\exp\left(-t^2/2\right)dt=\sqrt{2\pi}$. Undetermined coefficients can be obtained by integration:

$$A(x)=\frac{q}{2\pi\sigma_y\sigma_z}. \tag{7}$$

Substituting (3) into (1):

$$C(x,y,z)=\frac{q}{2\pi\sigma_y\sigma_z}\exp\left[-\frac{1}{2}\left(\frac{y^2}{\sigma_y^2}+\frac{z^2}{\sigma_z^2}\right)\right].$$

The diffusion coefficients σ_y and σ_z are related to the air stability and the vertical distance z, which increases with the increase of z. Therefore, the concentration of inert gas at each point in the coordinate range can be derived by Eq. (3). Since 1 m^3 air mass is about $V=1286$ g [14], the proportion of helium at any points can be obtained by substituting $\frac{C}{V}\times 100\%$, and then utilizing the oxygen content in the air, the proportion of oxygen at any points is $A\%=\left(1-\frac{C}{V}\right)\times 20\%$, so the oxygen concentration and proportion at any points can be calculated to explore whether it could satisfy the combustion-supporting conditions.

Laser heat transfer model

Laser is an electromagnetic radiation wave. The laser used for cutting is generally output in the mode of fundamental Gaussian mode. The cross-section spot is circular and the light intensity distribution basically satisfies the Gauss distribution. According to Professor Siegman's theory [15], heat flux density of laser heat source can be expressed as:

$$q(r)=\frac{3q_{\max}}{\pi w(z)^2}e^{\left(-\frac{3r^2}{w(z)}\right)}. \tag{8}$$

In this formula, *q(r)*—heat flux at radius R, W/mm^2; $q_{\max}$—the maximum value of heat flux density of laser beam, viz. the value at the center of beam waist radius, can be replaced by laser power value; *W(z)*—effective radius of beam at z coordinate, mm.

The beam passing through the lens will have a certain scattering, that is Rayleigh scattering. The divergence of the beam will cause a great impact on the heat transmission. The expression of the effective radius of the beam at the z coordinate is:

$$w(z)=w_0\sqrt{1+\left(\frac{z-z_0}{z_R}\right)^2} \tag{9}$$

where $w(z)$ is the Gaussian beam radius at the z coordinate, w_0 is the radius at the beam waist, z_0 is the ordinate at the beam waist, and z_R is the Rayleigh constant. Its value is determined by the scattering degree of the light source.

As there are no combustibles in the air, combustion would not occur even at high temperature, but the surface of processed wood is ablated by laser at high temperature. When the surface temperature is higher than the ignition point of wood and satisfied combustion-supporting conditions, combustion would occur on the surface of wood. Therefore, the boundary between combustion zone and non-combustion zone should be located on the processing surface of wood and perpendicular to the laser centerline. The thickness of wood processed by laser is only 2 mm, so the temperature drop caused by processing is ignored. The heat conduction rate between wood micro elements is roughly the same. Therefore, the heat transmitted at any two points perpendicular to the laser processing axis and equal to the vertical distance of the laser beam in the wood is the same. Meanwhile, the laser is a beam with concentrated energy and small scattering. Therefore, in the wood processed by laser, the heat conduction mode is primarily heat conduction, with small heat convection and ignoring the role of heat radiation. Together, along the direction perpendicular to the laser axis, the heat conduction can be described by the thermal conduction differential equation with constant physical properties, two-dimensional, unsteady state and internal heat source:

$$\frac{\partial T}{\partial t} = a\left(\frac{\partial^2 T}{\partial x^2} + \frac{\partial^2 T}{\partial y^2}\right) + \frac{\dot{\phi}}{\rho c} \tag{10}$$

In this formula, T—temperature, ℃; t—time, s; a—thermal diffusivity, $a = \frac{\lambda}{\rho c}$, m^2/s, taken as 1.7×10^{-7}; λ—thermal conductivity, W/(m·K), represented as 0.2; ρ—material density, kg/m^3, *Fraxinus mandshurica* signified as 686 kg/m^3; $\dot{\varphi}$—generation heat of heat source per unit volume, expressed as 6.67×10^{-10} J; c—specific heat of material, *Fraxinus mandshurica* indicated as 1.72×10^3 J/(kg·℃).

The transmission rate of laser heat in any direction of XOY plane is consistent. Therefore, a cylindrical coordinate system can be established in the heat diffusion direction. The two-dimensional heat transfer becomes a one-dimensional heat conduction problem along the radius direction. If the thermal conductivity of wood is a fixed value, the thermal conductivity differential equation can be expressed as:

$$\frac{d}{dr}\left(r\frac{dT}{dr}\right) = 0 \tag{11}$$

The indoor initial temperature is 18 ℃. Since the laser heating temperature is 1200 ℃ and the ignition point of wood is 280 ℃, when the temperature of mixed gas containing more than 12.5%, viz. above 280 ℃, wood would be ignited. Therefore, the initial conditions of this model are:

$$t = 0, \forall\, r \neq 0,\ t = \text{const} = 18\ ^\circ\text{C},$$

$$t = 0,\ r = 0,\ T = 1200\ ^\circ\text{C}.$$

When the oxygen concentration is higher than 12.5%, the mixed gas would burn. The oxygen content ratio of the mixed gas can be described by a certain boundary. In the XOY plane, its function expression is $y = f_1(x)$. When the temperature is lower than 280 ℃, the gas would not burn on the premise of sufficient oxygen content, and its boundary function expression is $y = f_2(x)$. Therefore, the boundary conditions of this model are exhibited as follows:

$$A\% = 12.5\%,\ y = f_1(x),$$

$$T = 356\ ^\circ\text{C},\ y = f_2(x),$$

$$y = f_1(x) \wedge f_2(x),$$

$$y = y_\infty, T = const,$$

$$h_0(T_\infty - T(r,t)) = -\lambda \frac{\partial T(r,t)}{\partial r}\bigg|_{r=r_0},$$

where h_0 is the convective heat transfer coefficient of the laser beam surface, and r_0 is the laser heating heat flow radius.

For the heat transfer process of laser processing, the comprehensive model is established as follows:

$$\begin{cases} \text{Jet equation: } q = 2q_0\left(\frac{R}{R_0}\right)^2 \frac{v_m}{v_0}\int_0^1 \left[1-\left(\frac{r}{R}\right)^{\frac{3}{2}}\right]^2 \frac{r}{R}d\left(\frac{r}{R}\right) \\ \text{Gas diffusion equation: } C(x,y,z) = \frac{q}{2\pi\sigma_y\sigma_z}\exp\left[-\frac{1}{2}\left(\frac{y^2}{\sigma_y^2}+\frac{z^2}{\sigma_z^2}\right)\right]; A\% = \left(1-\frac{C}{V}\right)\times 20\%, \\ \text{Heat source equation: } q(r) = \frac{3q_{\max}}{\pi w(z)^2}e^{\left(-\frac{3r^2}{w(z)}\right)}, \\ \text{Governing equation: } \frac{\partial T}{\partial t} = a\left(\frac{\partial^2 T}{\partial x^2}+\frac{\partial^2 T}{\partial y^2}\right)+\frac{\dot{\phi}}{\rho c}, \\ \text{Heat transfer equation: } \frac{d}{dr}\left(r\frac{dT}{dr}\right) = 0, \\ \text{Boundary condition: } A\% = 12.5\%, y = f_1(x);\ T = 356, \\ y = f_1(x)\wedge f_2(x). \end{cases}$$

Solution of model

Finite difference method

The finite difference method is to express the differential equation as a difference equation defined on discrete lattice points (i.e., the numerical relationship between lattice points reflected by the differential equation), and iteratively calculate the numerical value on the unknown boundary through the difference relationship between similar lattice points according to the given boundary conditions. The main difference between explicit and implicit difference methods is that the discretization approximate representation of differential terms in the difference equation instead of calculating differential equations is different, so that the explicit difference method can directly deduce the values on the target boundary from the known boundary conditions, while the implicit difference method constantly needs to solve the equations for recursive calculation. However, it elucidates that the results calculated by the difference method are not necessarily stable, and the small error may be amplified, resulting in the error of the calculation results.

To solve the partial differential equation problem by the finite difference method, the continuous problem must be discretized, namely, the solution area is meshed, the continuous solution area is replaced by a finite number of discrete grid nodes, and then the differential quotient of the partial differential equation is substituted by the difference quotient to derive the discretized difference equation system. Finally, the difference equations are solved by direct method or iterative method to achieve the numerical approximate solution of the differential equation.

When established the difference equations of heat conduction and gas diffusion, the solution area needs to be meshed by the internal node method. As shown in Fig. 2, the node temperature and gas concentration can approximately represent the temperature and gas concentration of the whole small area, which is convenient to deal with the uneven problem. Meanwhile, the data of boundary conditions are employed in the boundary points.

Assuming that in the grid, the time step τ, the space step along the x-axis direction h, the space step along the y-axis direction k, and the step along the radius direction n, the explicit difference scheme is used for discretization in this model to solve the temperature and gas concentration in the jth grid. The discretization scheme in the model is:

$$\begin{cases} \text{Jet equation: } q_j = 2q_0\left(\frac{R_j}{R_0}\right)^2 \frac{v_{mj}}{v_0}\int_{r_j-\frac{n}{2}}^{r_j+\frac{n}{2}} \left[1-\left(\frac{r_j}{R}\right)^{\frac{3}{2}}\right] \frac{r_j}{R}d\left(\frac{r}{R}\right), \\ \text{Diffusion equation: } C_j^n = \frac{q_j^n}{2\pi\sigma_{yj}^n\sigma_{zj}^n}\exp\left[-\frac{1}{2}\left(\frac{(y_j^n)^2}{(\sigma_{yj}^n)^2}+\frac{(z_j^n)^2}{(\sigma_{zj}^n)^2}\right)\right], \\ \text{Governing equation: } \frac{T_j^{n+1}-T_j^n}{\tau} = a_j\left(\frac{T_{j+1}^n-2T_j^n+T_{j-1}^n}{h^2}+\frac{T_{j+1}^n-2T_j^n+T_{j-1}^n}{k^2}\right)+\frac{\dot{\phi}_j}{\rho_j c_j}, \\ \text{Heat transfer equation: } \frac{T_j^{n+1}-T_j^n}{n}+r_j^n\frac{T_{j+1}^n-2T_j^n+T_{j-1}^n}{n^2} = 0. \end{cases}$$

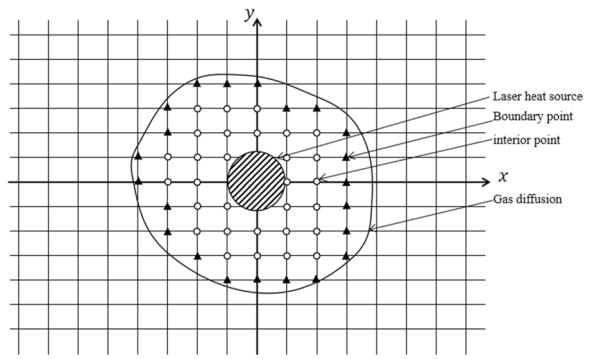

Fig. 2 Model meshing

For the explicit difference scheme, the discrete solution of unsteady heat transfer process needs to be considered in the stability condition. The above explicit difference formula displays that the temperature of the time node $n+1$ on the space node I is affected by the adjacent points on the left and right sides, and the stability limit condition (Fourier grid number limit) needs to be satisfied, otherwise there would be unreasonable oscillatory solutions[16].

$$\begin{cases} F_{O\Delta} = \frac{\lambda \Delta t}{\rho c (\Delta x)^2} \text{(grid number)}, \\ F_{O\Delta} \leq \frac{1}{2} \text{(inner node constraints)}, \\ F_{O\Delta} \leq \frac{1}{2\left(1+\frac{h\Delta x}{\lambda}\right)} \text{(boundary constraints)}. \end{cases}$$

After discretizing the unsteady process, the gas diffusion and heat transfer equations can be solved by the control equations and boundary conditions.

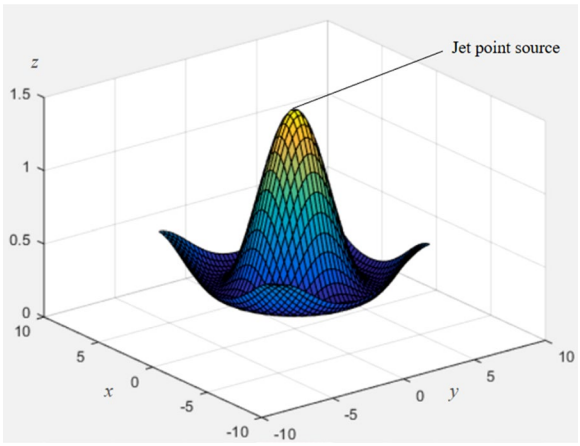

Fig. 3 Gas injection motion diagram

Solution of gas jet diffusion model

Under the idea of finite difference method, MathWorks Inc's MATLAB2015a software is employed to set the flow rate at the nozzle to 10 m/s and the height to 1 mm. The gas will expand due to energy absorption during injection. Meanwhile, the density of helium is less than that of air. After leaving the nozzle, helium will be subjected to the air buoyancy, resulting in an upward trend, which would further lead to the expansion of the outer diameter of the gas. The distribution of gas trajectory after helium is injected out of the nozzle is shown in Fig. 3.

After the gas is injected through the nozzle, the instability of the gas itself will diffuse and the concentration of helium will decrease along the X and Y directions. The

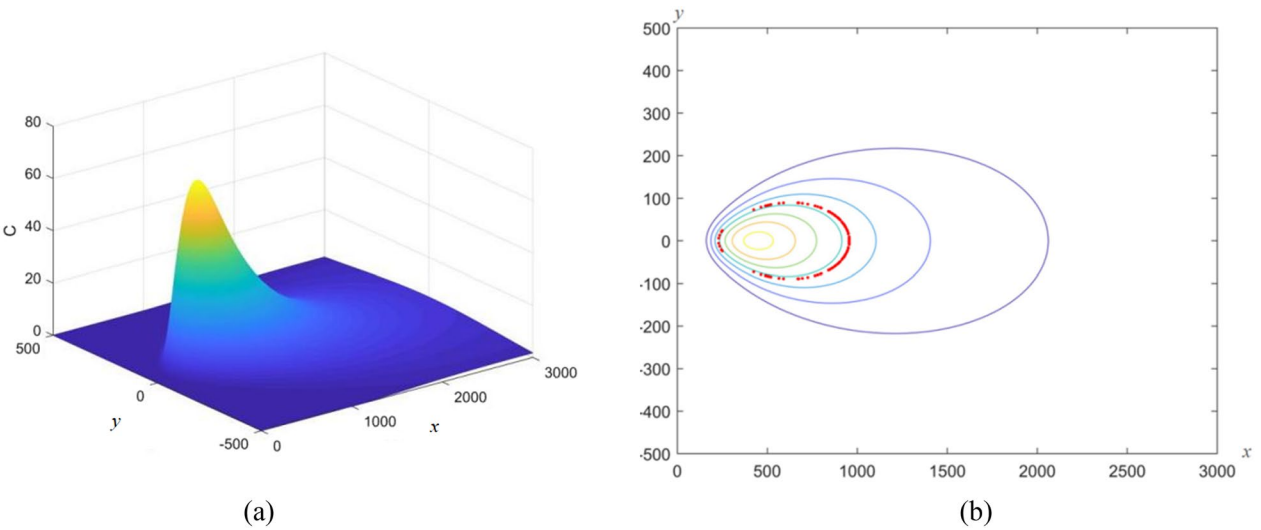

Fig. 4 **a** Gas diffusion concentration distribution. **b** Isoconcentration diagram of gas diffusion in XOY plane

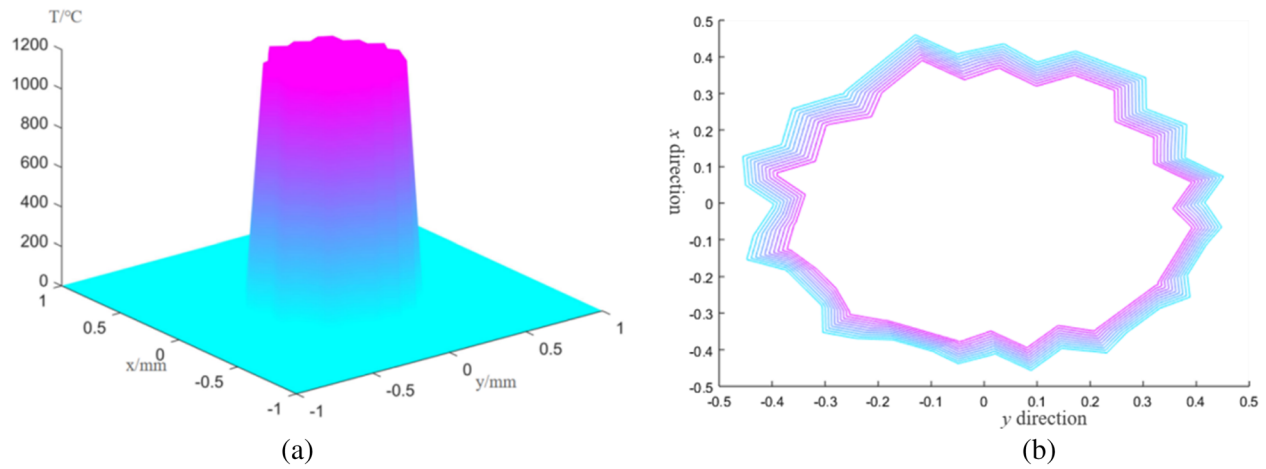

Fig. 5 .**a** Wood surface temperature distribution. **b** Wood surface isotherm

greater the helium concentration is, the smaller the air concentration is. Therefore, along a fixed direction, the gas will diffuse with the flow, and the concentration will gradually decrease during diffusion, resulting in the gradual increase of oxygen content. Therefore, the proportion of oxygen can be achieved by helium concentration. The distribution of helium diffusion concentration is shown in Fig. 4a:

The proportion of oxygen in the air is about 20% and combustion support can be realized when the oxygen content is higher than 12.5%. When the oxygen content is 12.5%, the proportion of air is 62.5%, and the helium concentration is 37.5%. Therefore, when the helium concentration is 37.5%, other gases can realize combustion support. The concentration distribution line of gas diffusion is shown in Fig. 4b, in which the red dotted line is the isoconcentration line of helium concentration of 37.5%. When the oxygen concentration is higher than 12.5%, the combustion-supporting effect can be realized.

Solution of laser heat transfer model

According to the assumptions, the laser heating temperature does not decrease with the processing depth, and the wood is a poor conductor with low thermal conductivity. Meanwhile, the wood is an anisotropic material with significant differences in porosity, moisture content and other physical properties. Combustion would occur when the wood surface temperature is higher than its ignition point of 280 ℃, but due to the anisotropy of the wood material, the heat conduction efficiency in each direction is different. When the moisture content in one direction is high, the heat transfer efficiency of wood

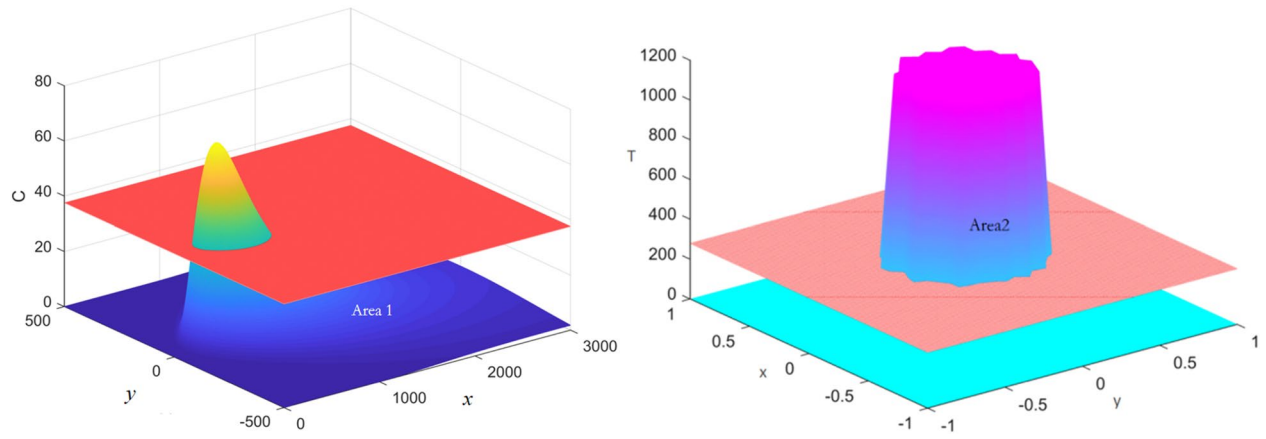

Fig. 6 Machining plane combustion zone

will also enhance. Set the wood performance parameter as the original wood parameter, and take the processing time $t=2$ s to achieve the wood surface temperature distribution, as shown in Fig. 5a.

As the thermal conductivity of wood is relatively poor, the temperature decreases rapidly during heat transfer. In addition, Fraxinus mandshurica is composed of fiber structure, and the transverse and longitudinal thermal conductivity are quite different. Due to the influence of wood fiber structure, the carbon content in the along-grain cutting mode is significantly less than that of the cross-grain cutting mode, whereas the thermal conductivity of longitudinal fiber and transverse wood cells are also very small. Therefore, the temperature drop on the wood surface changes rapidly with coordinates. Chosen various temperature and laser source as the origin, a plane rectangular coordinate is established on the processing surface. The factors affecting heat conduction such as porosity and moisture content on the wood surface are randomly distributed, and the isotherm is shown in Fig. 5b.

The feasible areas of gas concentration and temperature are shown in Fig. 6. Selected 37.5% to mark the critical line of combustion-supporting gas in the concentration change diagram. The oxygen content in the area outside the critical line (marked as area 1) can achieve the combustion-supporting effect. The temperature of 280 ℃ is selected to mark the isotherm on the wood surface. The wood may burn in the inner area of 280 ℃ (marked as area 2), and the intersection area of areas 1 and 2 will produce combustion and forming a combustion area.

It can be signified from the above figures that the oxygen content of the machining surface would be reduced after adding helium, which destroys the combustion conditions. As such, when using inert gas-assisted laser processing, the carbide generated by combustion will be reduced, the slit width declined correspondingly, and the machining accuracy as well as cutting quality will be further improved.

Materials and methods

In the process of inert gas-assisted laser processing wood, the slit quality is the standard to evaluate the forming process. Due to the absorption of laser energy, heat conduction and mass flow under the pressure of auxiliary gas, the process of gas-assisted laser processing is quite complex. The selection of various parameters would have a vital impact on the cutting quality.

Materials

According to the experimental requirements, the selected cherry wood veneer was processed into a certain size when purchased, and its specification was 120 mm × 80 mm × 5 mm. The moisture content was 15%, and the surface of the plate was flat and smooth without cracks, defects, knots, decay and other defects. In order to ensure the smooth progress of the experiment and the feasibility of the later test, the wood surface was sanded with 240# sandpaper in the early stage of the experiment. As the wood is a typical anisotropic porous medium material, when cutting along fiber, the laser beam passes through the aggregate of countless fiber bundles. While cutting across grain, the laser beam passes through the thin-walled cavity tissue composed of wood rays. Due to the differences of structures, the cutting seam sizes in different cutting directions are inconsistent. Therefore, both the along-grain direction and the cross-grain direction should be considered during processing. Thus, the influence experiment of process parameters on wood cutting quality is studied. Taking the slit width and surface roughness as evaluation indexes, the influence laws of traditional laser cutting and gas-assisted laser cutting in different texture directions are compared and analyzed to acquire the optimal processing method. Therefore, both along the grain direction and across the grain direction should be considered during processing.

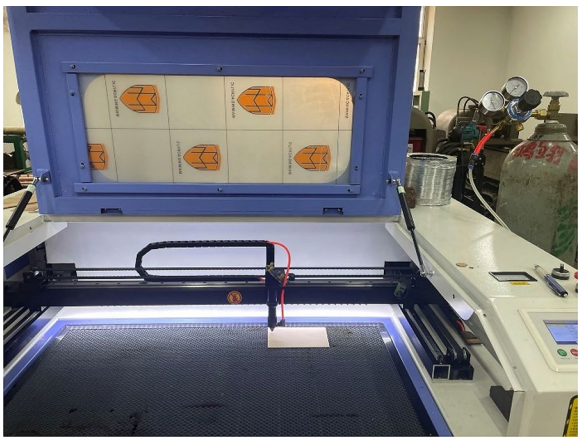

Fig. 7 Gas-assisted laser processing equipment

In this study, helium is progressively proposed to be employed as the inert gas for auxiliary laser processing. The equipment used in the forming test of inert gas-assisted laser processing of wood is the laser cutting machine produced by Shandong baomei, as shown in Fig. 7.

The wavelength of CO_2 laser is 10.6 μm, the rated power of laser is 80 W, and the focal length of lens is 63.5 mm. Industrial helium with purity ≥ 99.999% is selected as the inert gas. After pressure regulation and stabilization through the pressure reducing valve, it

Table 1 Cherry wood processing parameters by inert gas-assisted laser

Process parameters	1	2	3	4	5	6	7
Laser power(W)	30	35	40	45	50	55	60
Cutting speed(mm/s)	25						
Gas pressure(MPa)	0/0.1						

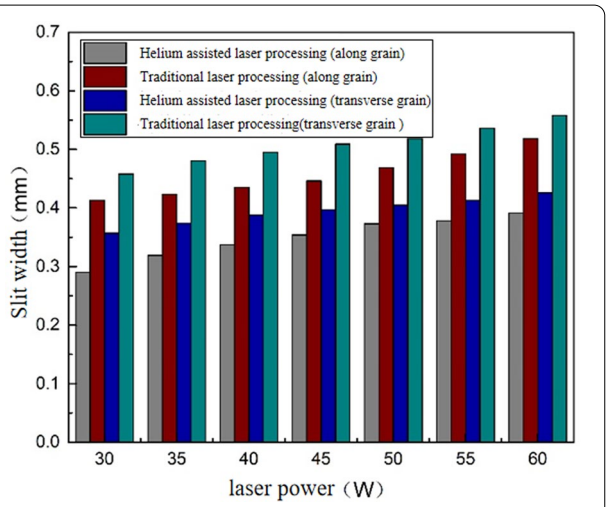

Fig. 8 Influence of laser parameters on the width of kerf during grain cutting

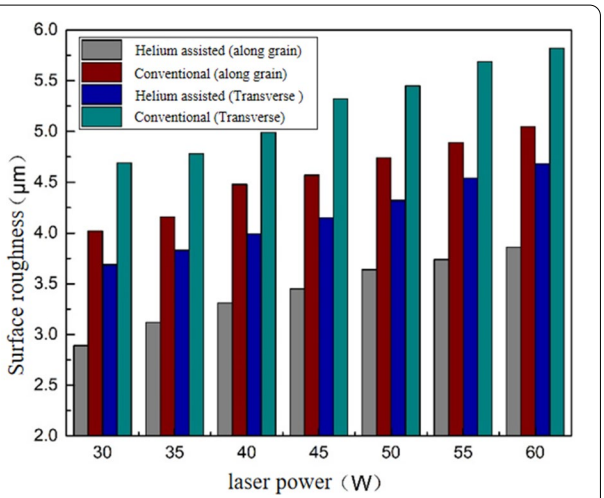

Fig. 9 Influence of laser parameters on surface roughness during transverse cutting

enters the nozzle from the air duct and is sprayed coaxially with the laser beam to the surface of wood. The gas pressure at the nozzle can reach 2.5 MPa at most. Table 1 exhibits specific process parameters for selecting.

After laser ablation of cherry wood, Quorum Q150t PLUS automatic high vacuum sputtering instrument of Nanjing Qinsi Technology Co., Ltd is proposed. The uniformity of gold spraying determines the image clarity during SEM observation, so it is necessary to ensure uniform coating and reasonable thickness. The Apreo scanning electron microscope produced by Thermo Scientific Company of the United States is used to measure and analyze the wood cutting surface processed by inert gas-assisted laser. The micromorphology of the slit surface is examined, and the surface composition of the slit surface is analyzed by energy spectrum analysis. The slit width and depth are measured by MOTIC Co., Ltd's BA400 microscope. The distance from the top to the bottom of the slit can be measured as the slit depth. In order to ensure the accuracy of the measurement results, each incision should be measured repeatedly three times and expressed by the average value.

Cutting quality analysis

In the process of cutting, we usually think that under the same processing conditions, the smaller the slit width and the lower the roughness at the slit are, the higher the cutting quality is. Therefore, this paper aims to analyze and evaluate the cutting quality with the slit width and slit surface roughness as the evaluation criteria. Figure 8 exhibits the influence of laser process parameters on slit width under two modes of traditional laser processing and inert gas-assisted laser processing. When the cutting speed is constant, whether there is helium or not, the change trend of slit width under different laser power is basically similar, and the slit width enhances with the increase of laser power. When the laser power is low, it can be derived from Eq. (8) that the heat flux generated by the laser decreases, and less heat is transmitted by the bad conductor, so a narrow slit will be formed. Reversely, when the power is relatively high, the heat flux increases, and the ablation area of the laser on the machined surface also enhances, which makes the slit width larger.

Compared with the traditional laser processing, the slit width of the plate with the assistance of inert gas is significantly smaller than that without the assistance of inert gas. As the auxiliary gas, helium effectively affects the

combustion-supporting conditions of the machined surface, making the combustion area smaller and the ablation as well as carbonization part at the slit reduced. The experimental results reveal that when the laser power is 30 W and the cutting speed is 25 mm/s, the longitudinal slit of traditional laser processing is 0.42 mm and the minimum width of longitudinal slit of gas-assisted laser processing is 0.29 mm. Gas-assisted laser processing has the advantages of reducing slits and enhancing cutting quality.

In addition, the roughness of cutting seam is also one of the important indicators to measure the quality of cutting seam. Therefore, according to relevant standards [17],we use *Ra* to characterize the surface roughness of the machined surface. We measure the surface roughness with the aid of a slit tester. The lower the surface roughness can make the higher the cutting quality. In traditional laser processing and inert gas-assisted laser processing, the influence of laser parameters on surface roughness under two modes of along-grain cutting and cross-grain cutting is shown in Fig. 9. When the cutting speed is constant, the change trend of surface roughness under various laser power is generally similar, and the surface roughness increases with the increase of laser power. This is due to the laser power small, the laser energy interacted on the processed surface for heat transfer is small. The ablation ability of wood at the slit is weakened, the flatness of the slit surface is excellent, and the surface roughness is small. When the laser power increases, the heat transferred by the laser to the direction perpendicular to the laser axis enhances, and the corresponding area of carbonization and ablation also increases. When helium assisted laser processing, helium hinders the ablation effect of laser on the surface. The heat in the ablation area in the slit and the residue generated by incomplete gasification are taken away by gas purging, so that these heat cannot be further transmitted to the interior of the workpiece, which reduces the heat accumulation temperature, effectively reduces the heat affected zone, and reduces the ablation amount of wood. Therefore, the slit width is relatively small and the slit parallelism is relatively good. The experiments elucidate that when the laser power is 30 W and the cutting speed is 25 mm/s, the minimum surface roughness along the grain of wood processed by gas-assisted laser is $Ra = 2.89$ μm. The minimum cross-grain surface roughness of gas-assisted laser processing wood is $Ra = 3.69$ μm. As seen therein, helium-assisted laser processing can effectively improve the processing quality and reduce the surface roughness dramatically.

Table 2 Factors and levels of inert gas-assisted laser processing of wood

Factor	Process parameters	Factor level		
		-1	0	1
x_1	Laser power(W)	40	45	50
x_2	Cutting speed(mm/s)	22	24	26
x_3	Gas pressure(MPa)	0.10	0.15	0.20

Response surface methodology

Response surface methodology (RSM) is a method for optimizing experimental conditions. A reasonable experimental design method is employed to obtain certain data. By studying the influence of the interaction between various factors in the response, the multiple quadratic regression equation is conducted to fit the functional relationship between the factors and the response value, and the response value of each factor level is acquired. Afterwards, the optimal value of the predicted response and the experimental conditions of the response were found out.

The response variables of laser cutting of wood are yielded and processing quality. The former is expressed by the maximum slit depth reached in the cutting process, and the latter is related to slit width and surface roughness. In the response surface method, the Box–Behnken design experimental design is an experimental design that can evaluate the nonlinear relationship between indicators and factors. It is a typical rotatable design method. Based on the above single factor test results, the response surface method experiment is carried out with laser power (x_1), cutting speed (x_2) and air flow pressure (x_3) as parameters. The factors and levels of inert gas-assisted laser wood processing test are shown in Table 2.

In the response surface problem, the mathematical model of each response is obtained through multiple linear regression analysis, and the approximation function between the response variable y and the control variable x is established. The significance level of the variables in the model is determined through variance analysis, and the coefficients of the multiple regression model are estimated by the least square method. The second-order model is below:

$$y = \beta_0 + \sum_{i=1}^{k} \beta_i x_i + \sum_{i=1}^{k} \beta_{ii} x_i^2 + \sum_{i<j} \sum \beta_{ij} x_i x_j + \varepsilon \tag{12}$$

In the above formula: y—predicted response value; β_0—constant term; β_i—main effect coefficient; β_{ii}—secondary effect coefficient; β_{ij}—interaction term absorption.

Table 3 Box–Behnken matrix and response values

Serial number	Factor			Response value		
	Laser power (W)	Cutting speed (mm/s)	Gas pressure (MPa)	Slit width (mm)	Slit depth (mm)	Surface roughness (μm)
1	45	22	0.20	0.37	3.02	3.27
2	45	24	0.15	0.34	2.43	3.02
3	40	26	0.15	0.29	2.27	1.72
4	50	24	0.20	0.39	3.34	3.39
5	45	24	0.15	0.34	2.45	3.04
6	45	26	0.20	0.33	2.81	2.50
7	50	26	0.15	0.36	2.97	2.76
8	40	24	0.10	0.32	1.95	1.83
9	50	22	0.15	0.43	3.58	3.48
10	45	22	0.10	0.39	2.68	2.69
11	40	24	0.20	0.30	2.59	2.02
12	50	24	0.10	0.42	3.13	2.92
13	45	24	0.15	0.35	2.46	3.04
14	45	24	0.15	0.34	2.48	4.07
15	45	26	0.10	0.36	2.16	2.36
16	40	22	0.15	0.30	2.35	2.11
17	45	24	0.15	0.34	2.49	3.08

Table 4 Variance analysis of kerf width regression model

Variation source	Sum of squares	Freedom	Mean square	*F* value	*P* value
Model	0.0253	9	0.0028	187.2000	< 0.0001
x_1	0.0190	1	0.0190	1267.5000	< 0.0001
x_2	0.0028	1	0.0028	187.5000	< 0.0001
x_3	0.0012	1	0.0012	83.3300	< 0.0001
x_1x_2	0.0009	1	0.0009	60.0000	0.0001
x_1x_3	0.0000	1	0.0000	1.6700	0.2377
x_2x_3	0.0000	1	0.0000	1.6700	0.2377
x_1^2	4.211×10^{-6}	1	4.211×10^{-6}	0.2807	0.6126
x_2^2	0.0001	1	0.0001	4.4900	0.0718
x_3^2	0.0011	1	0.0011	76.4200	< 0.0001
Residual	0.0001	7	0.0000		
Spurious term	0.0000	3	8.333×10^{-6}	0.4167	0.7510
Error	0.0001	4	0.0000		
The sum	0.0254	16			

Response surface regression model

Table 3 displays the experimental results of response surface method for inert gas-assisted laser processing of wood. Taking slit width, slit depth and surface roughness as evaluation indexes, the mathematical models of three response parameters: laser power, cutting speed and air flow pressure are established.

The quadratic polynomial function is used to describe the predicted response of slit width, slit depth, surface roughness and process parameters in this experiment:

$$\begin{aligned} y_{\text{width}} = &- 0.96825 + 0.05085x_1 + 0.013875x_2 \\ &- 1.18x_3 - 0.0015x_1x_2 - 0.01x_1x_3 \\ &- 0.025x_2x_3 - 0.00004x_1^2 + 0.001x_2^2 + 6.6x_3^2, \end{aligned} \tag{13}$$

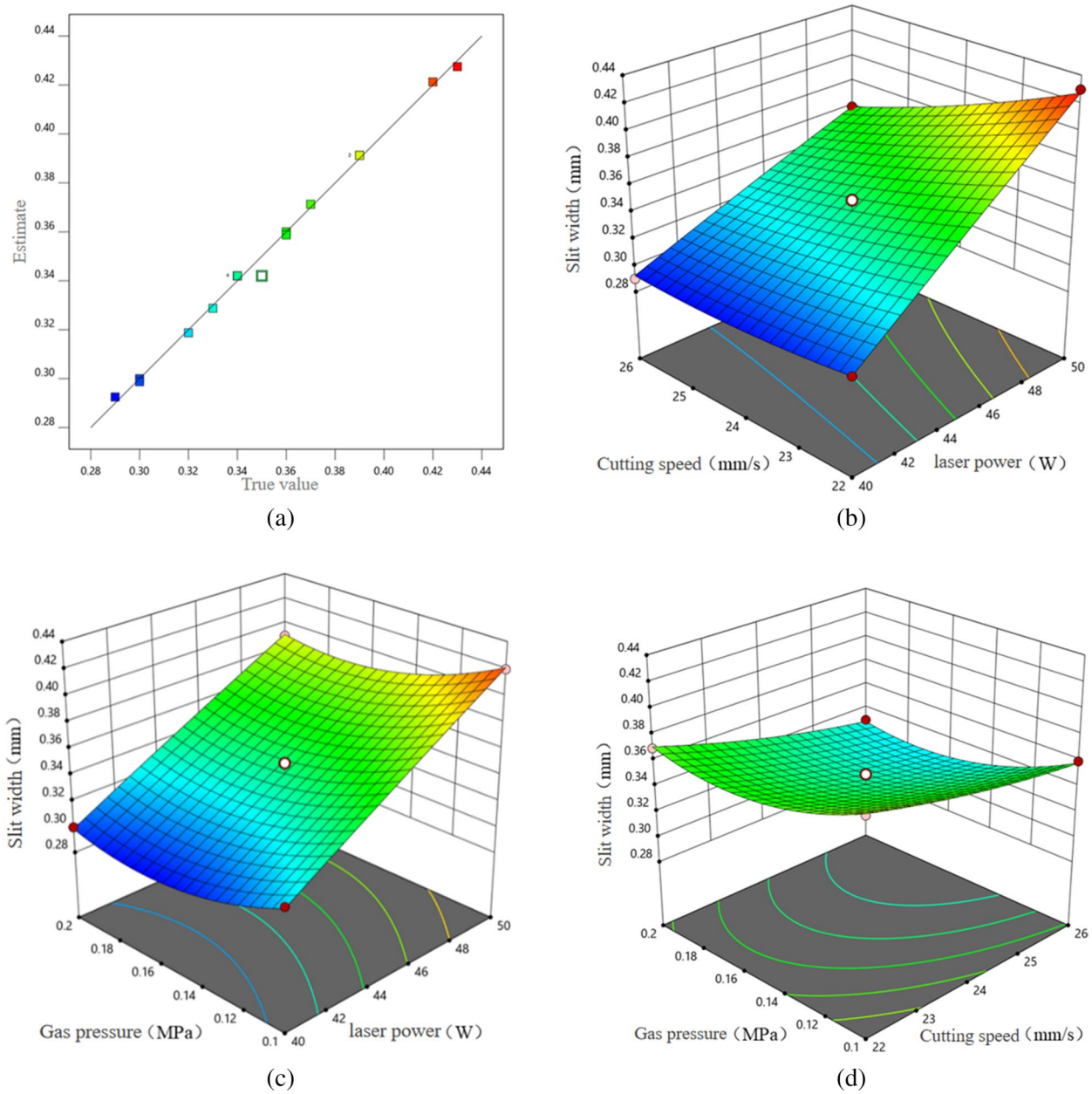

Fig.10 Response surface diagram of cutting width of inert gas-assisted laser cutting wood. **a** Comparison between predicted and actual. **b** Interaction of laser power and cutting speed. **c** Interaction of laser power and gas pressure. **d** Interaction of cutting speed and gas pressure

$$\begin{aligned} y_{\text{depth}} =& 20.3855 - 0.2689x_1 - 1.08175x_2 \\ & - 4.58x_3 - 0.01325x_1x_2 - 0.43x_1x_3 \\ & + 0.775x_2x_3 + 0.00831x_1^2 \\ & + 0.030688x_2^2 + 33.1x_3^2, \end{aligned} \tag{14}$$

$$\begin{aligned} y_{\text{Ra}} =& -67.00325 + 1.53685x_1 + 2.61512x_2 \\ & + 36.72x_3 - 0.00825x_1x_2 + 0.28x_1x_3 \\ & - 1.1x_2x_3 - 0.001399x_1^2 \\ & - 0.046187x_2^2 - 64.9x_3^2. \end{aligned} \tag{15}$$

Table 5 Variance analysis of kerf depth regression model

Variation source	Sum of squares	Freedom	Mean square	*F* value	*P* value
Model	2.9800	9	0.3310	469.93	< 0.0001
x_1	1.8600	1	1.8600	2644.45	< 0.0001
x_2	0.2520	1	0.2520	357.88	< 0.0001
x_3	0.4232	1	0.4232	600.89	< 0.0001
x_1x_2	0.0702	1	0.0702	99.71	< 0.0001
x_1x_3	0.0462	1	0.0462	65.63	< 0.0001
x_2x_3	0.0240	1	0.0240	34.11	0.00006
x_1^2	0.1817	1	0.1817	258.03	< 0.0001
x_2^2	0.0634	1	0.0634	90.08	< 0.0001
x_3^2	0.0288	1	0.0288	40.94	0.0004
Residual	0.0049	7	0.0007		
Spurious term	0.0027	3	0.0009	1.55	0.3325
Error	0.0023	4	0.0006		
The sum	2.9800	16			

In this formula: y—Response value; x_1—laser power; x_2—cutting speed; x_3—gas pressure.

Influence of interaction of process parameters on slit width

The variance analysis and significance test of the slit width test results in the process of inert gas-assisted laser cutting wood are described in Table 4 to evaluate the reliability of the test results. P indicates the significance of each item in the model. Among the effects of the primary item, the laser power has the most significant effect on the slit width, followed by the cutting speed and air flow pressure. The interaction between various factors is more significant.

Figure 10 is the response surface of slit width under different parameter combinations of inert gas-assisted laser cutting wood. It can be observed from Fig. 10a that the interaction of process parameters has a significant impact on the slit width. Most of the experimental values are distributed above the predicted values, and the predicted values of the established model are in good agreement with the experimental values. Figure 10b demonstrates the influence of the interaction of laser power and cutting speed on the slit width. As the laser energy is transmitted downward on the surface of the machined surface, when the cutting speed at low water level, the excess laser energy heats the flue gas and burned products in the incision to produce a large slit. With the increase of laser power, more laser energy accumulates on the wood surface, and the influence on the slit width enhances significantly. Figure 10c elucidates the influence of the interaction of laser power and airflow pressure on the slit width. Larger laser power and lower airflow pressure lead to the enhancement of wood slit width, and the influence of laser power on the slit width is more significant than that of airflow pressure. Figure 10d signifies the effect of the interaction between cutting speed and air flow pressure on the slit width. The interaction between air flow pressure and cutting speed has no obvious effect on the slit width, as the interaction time between gas jet and wood surface is prolonged, higher auxiliary gas pressure enhanced the cooling effect in the laser action zone. In what follows, the uneven pressure and temperature in the gas flow will cause the change of gas flow field density and change the energy impact of the laser beam and the energy distribution along the material notch. According to the corresponding experimental results of various influencing factors, the optimal conditions for obtaining the minimum slit width of wood by inert gas-assisted laser processing are listed as follows: laser power 40 W, cutting speed 25.15 mm/s, gas pressure 0.17 MPa, and the minimum slit width is 0.29 mm.

Influence of process parameter interaction on cutting seam depth

The variance analysis and significance test of the experimental results of slit depth in the process of inert gas-assisted laser cutting wood are recorded in Table 5. Among the primary effects, the laser power has the most significant effect on slit depth, followed by air flow pressure and cutting speed. The interaction between laser power and cutting speed and the interaction between laser power and airflow pressure also have a significant impact on the slit depth. This is due to the fact that the formation of the slit of the workpiece is primarily caused

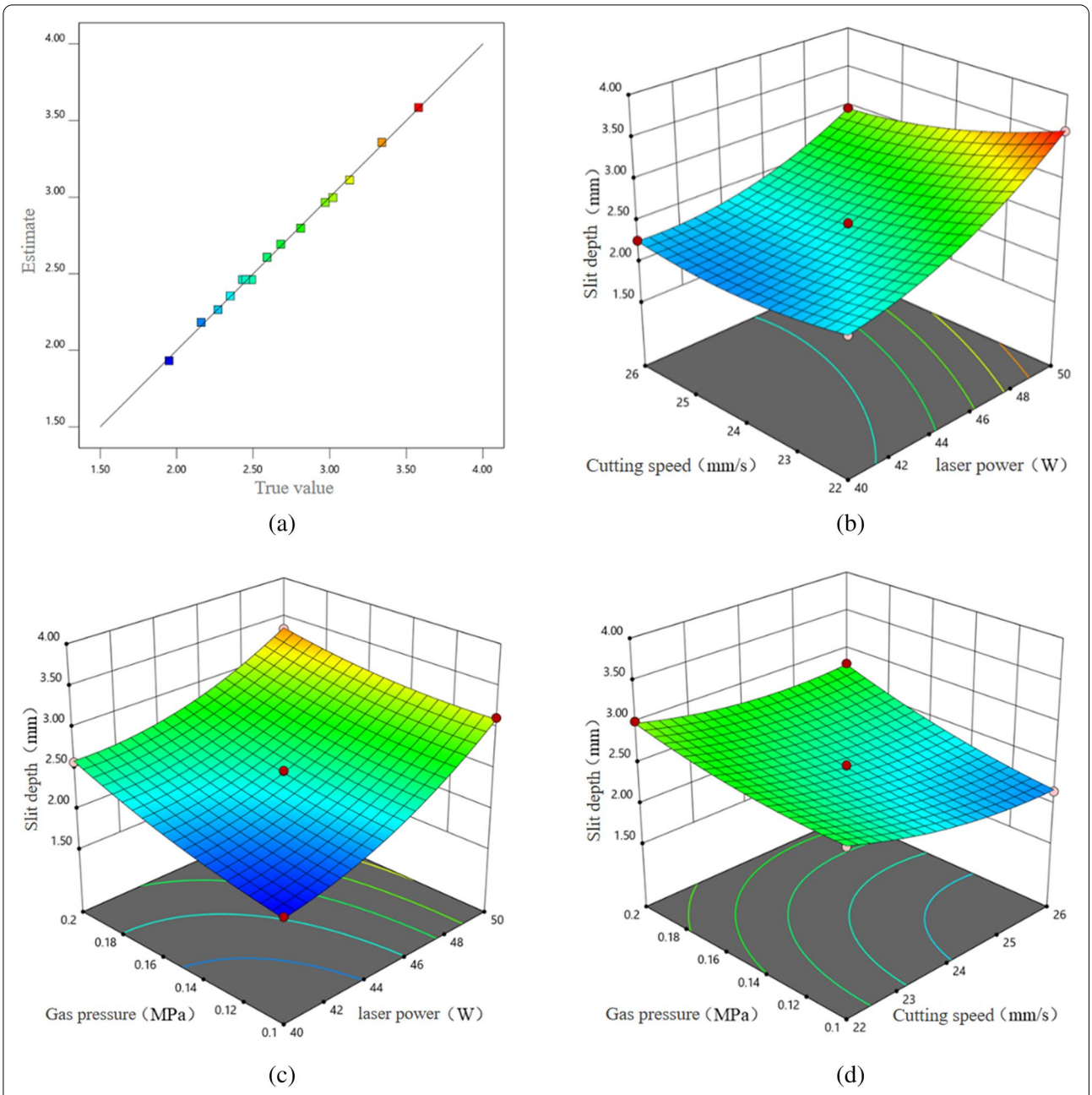

Fig. 11 Response surface diagram of cutting depth of inert gas-assisted laser cutting wood. **a** Comparison between predicted and actual. **b** Interaction of laser power and cutting speed. **c** Interaction of laser power and gas pressure. **d** Interaction of cutting speed and gas pressure

by the combustion and heat accumulation. As such, when the laser power is large, the slit depth increases. When the cutting speed increases, the slit depth decreases due to the short action time and less heat accumulated on the wood surface.

Figure 11 is the response surface of slit depth under the combination of parameters of inert gas-assisted laser cutting wood. Figure 11b demonstrates the influence of the interaction between laser power and cutting speed on the cutting depth. Since the laser cutting of wood primarily depends on the thermal process of laser beam providing energy, when the cutting speed is at a low level, the energy for transmission enhances with the gradual increase of laser power, and the enhanced coupling between laser beam and material will produce deeper cutting. Figure 11c reveals the influence of the

Table6 Variance analysis of surface roughness regression model

Variation source	Sum of squares	Freedom	Mean square	*F* value	*P* value
Model	4.7500	9	0.5282	1210.27	< 0.0001
x_1	2.9600	1	2.9600	6792.89	< 0.0001
x_2	0.6105	1	0.6105	1398.88	< 0.0001
x_3	0.2381	1	0.2381	545.45	< 0.0001
x_1x_2	0.0272	1	0.0272	62.38	< 0.0001
x_1x_3	0.0196	1	0.0196	44.91	0.0003
x_2x_3	0.0484	1	0.0484	110.90	< 0.0001
x_1^2	0.5151	1	0.5151	1180.15	< 0.0001
x_2^2	0.1437	1	0.1437	329.30	< 0.0001
x_3^2	0.1108	1	0.1108	253.98	< 0.0001
Residual	0.0031	7	0.0004		
Spurious term	0.0008	3	0.0003	0.45	0.7292
Error	0.0023	4	0.0006		
The sum	4.7600	16			

interaction of laser power and gas flow pressure on the slit depth. At a higher laser power level, the laser energy is evenly distributed along the thickness direction of the workpiece. With the increase of gas jet pressure, the scouring effect is enhanced, which is conducive to remove particle smoke and combustion particles in the slit and reduces the residues in the slit. The propagation of laser beam in the slit is smoother and the slit depth is increased. Figure 11d shows the influence of the interaction between cutting speed and air pressure on the cutting depth. Under the condition of low cutting speed, affected by the action time of gas jet impacting wood, the longer impact process will produce higher kinetic energy, exert greater shear stress on the cutting wall, and then increase the cutting depth. Based on the experimental results, the optimal conditions for the maximum seam depth of wood processed by inert gas-assisted laser are: laser power 50 W, cutting speed 22 mm/s, gas pressure 0.15 MPa, and the maximum seam depth is 3.58 mm.

Influence of process parameter interaction on surface roughness

The variance analysis and significance test of the experimental results of surface roughness in the process of inert gas-assisted laser cutting wood are listed in Table 6. Among the primary effects, the laser power possesses the most significant effect on the cutting depth, followed by the cutting speed and air flow pressure. Thereafter, the interaction between laser power and cutting speed also has a significant influence.

Figure 12 elaborates the response surface of surface roughness under various parameters combinations of inert gas-assisted laser cutting wood. Figure 12b exhibits the effect of the interaction of laser power and cutting speed on surface roughness. In the selected parameter range, when the cutting speed at a low level, the slit surface roughness enhances with the increase of laser power and produces a large rate. It is suggested that the interaction between cutting speed and laser power have a great influence on the surface roughness of slit after cutting. When the laser power increases, more heat accumulates on the wood cutting surface, resulting in the increase of cutting seam surface roughness. Figure 12c demonstrates the effect of the interaction between laser power and air flow pressure on surface roughness. Lower laser power combined with low pressure could acquire smaller surface roughness, which is primarily due to the excellent distribution of laser energy along the cutting depth direction and lower shear stress of jet. The combination of high laser power and high air flow pressure have the higher surface roughness, as the gas jet exerts a higher shear force, which makes the machined surface rougher. Figure 12d demonstrates the effect of the interaction between cutting speed and air flow pressure on surface roughness. The surface roughness enhances with the increase of air flow pressure, as with the increase of gas jet pressure, more materials are eliminated from the slit by the generated shear force, and the adhesion of combustion products attached to the surface of wood after carbonization is poor. Therefore, it will have a significant impact on the surface roughness. According to

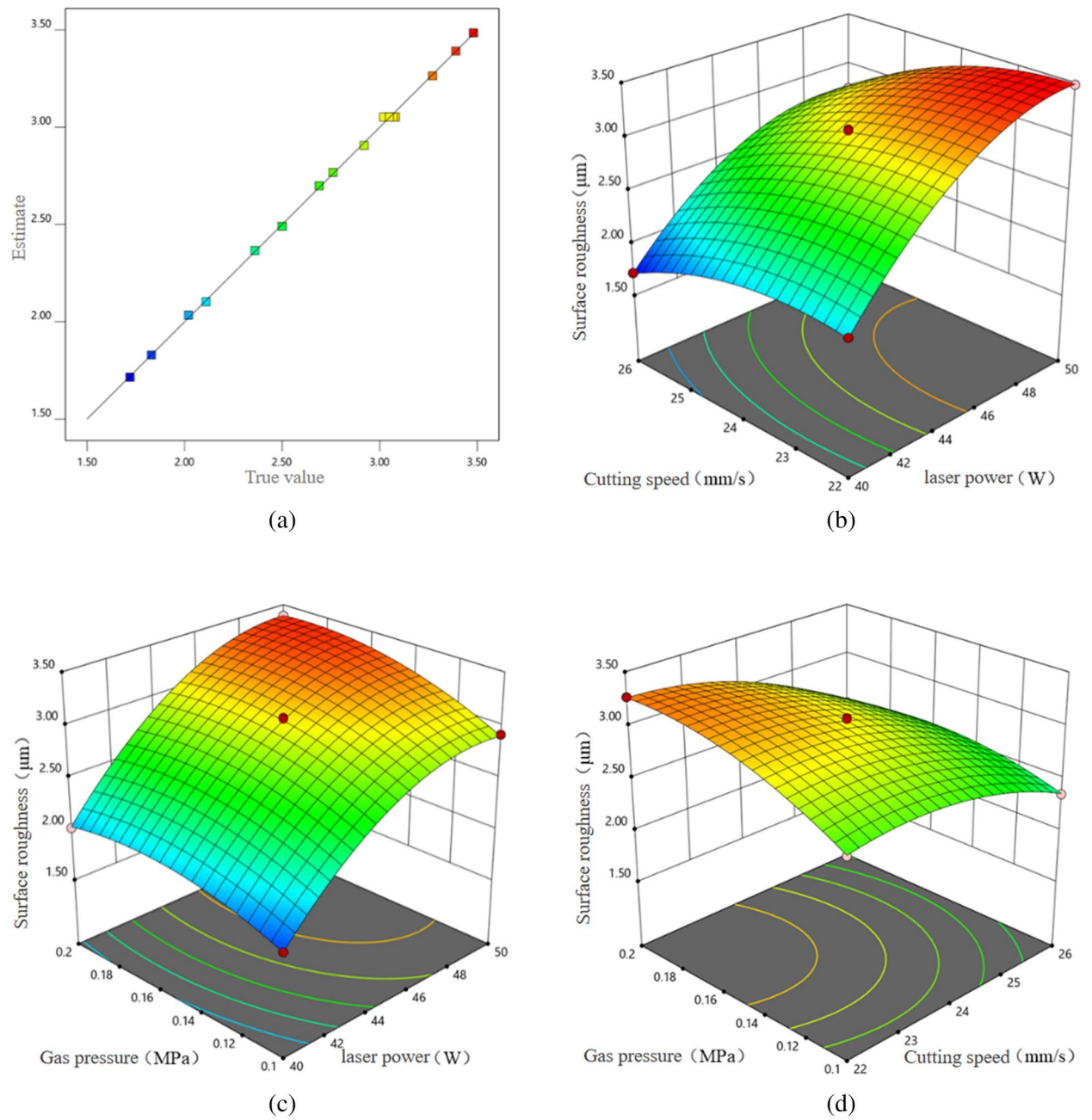

Fig.12 Response surface diagram of surface roughness of inert gas-assisted laser cutting wood. **a** Comparison between predicted and actual. **b** Interaction of laser power and cutting speed. **c** Interaction of laser power and gas pressure. **d** Interaction of cutting speed and gas pressure

the corresponding experimental results of various influencing factors, the optimal conditions for obtaining the surface roughness of wood assisted by inert gas laser processing are: laser power 40 W, cutting speed 25.99 mm/s, gas pressure 0.15 MPa, and the minimum surface roughness is 1.72 μm.

Process parameter optimization

The objective of selecting process parameters of inert gas-assisted laser cutting is to obtain the minimum slit width, maximum slit depth and minimum surface roughness under reasonable process conditions. The optimized process parameters maximize the process range and the quality of cutting section, but each parameter level is

Table 7 Variation range and importance of inert gas-assisted laser wood processing parameters

Process parameters	Target	Minimum	Maximum	Importance
Laser power (W)	Within range	40	50	5
Cutting speed (mm/s)	Within range	22	26	3
Gas pressure (MPa)	Within range	0.1	0.2	1
Slit width (mm)	Minimum	0.29	0.43	3
Slit depth (mm)	Maximum	2.51	3.58	3
Surface roughness (μm)	Minimum	2.79	3.98	5

Table 8 Selection and verification of model process parameters

Evaluation criterion	Selection of process parameters				Error (%)
	Laser power (W)	Cutting speed (mm/s)	Gas pressure (MPa)		
Minimum slit width (mm)					
Estimate	40	25.153	0.167	0.289	0.35
Actual value	40	26.000	0.150	0.290	
Maximum cutting depth (mm)					
Estimate	50	22.000	0.150	3.585	0.14
Actual value	50	22.000	0.150	3.580	
Minimum surface roughness (μm)					
Estimate	40	25.991	0.150	1.718	0.12
Actual value	40	26.000	0.150	1.720	

independent each other. Selecting process parameters, it is difficult to acquire the minimum surface roughness which meets the maximum cutting seam depth. Therefore, it is necessary to optimize and verify according to the importance of each parameter. Table 7 elaborates the variation range and importance index of inert gas-assisted laser processing process parameters.

Table 7 lists the representation of each response weight and its importance, from 1 to 5 (the importance reaches from small). The weight of each response is a process of yield and quality prediction based on a priority. The weight of each parameter is determined by its frequency as an important parameter or its participation in the interaction affecting the analyzed response.

The optimal combination of process parameters for inert gas-assisted laser processing of wood is described in Table 8. These process parameters achieve the target requirements of each response and maximize the process quality of laser cutting. It can be observed that the predicted value of the model is basically consistent with the experimental value, and the error is small. Under three different evaluation criteria, the error of slit width is 0.35%, and the errors of slit depth and surface roughness are 0.14% and 0.12%, respectively. The experimental results substantiate that the model prediction value of surface roughness is the best.

Figure 13 shows the cutting quality of inert gas-assisted laser processing wood when the laser power is 40 W, the cutting speed is 26 mm/s and the gas pressure is 0.15 MPa. It can be discovered from Fig. 13a that the cutting seam quality obtained by traditional laser cutting wood is poor, a large amount of residue

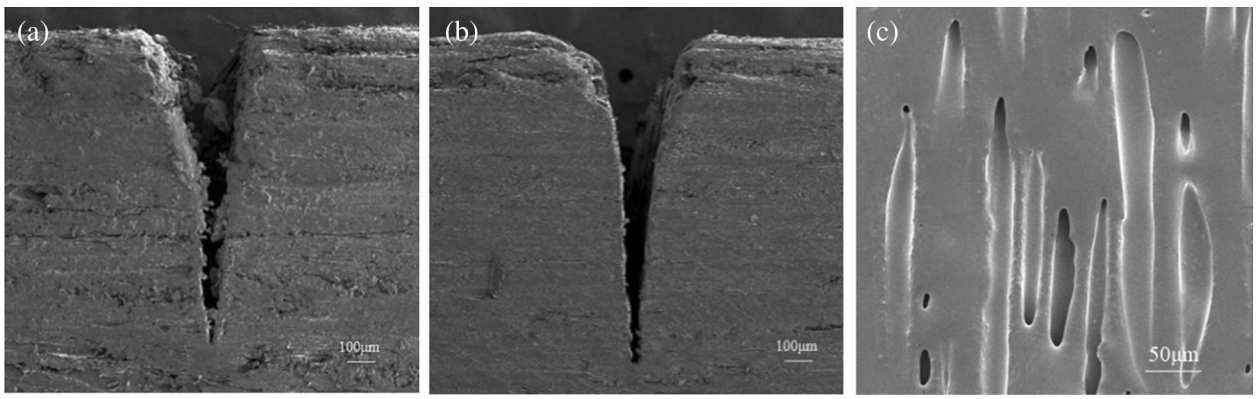

Fig. 13 Gas-assisted laser cut wood surface optimization. **a** Traditional laser machining. **b** Gas-assisted laser processing. **c** Micromorphology of kerf surface

accumulation generated at the bottom of the cutting seam, and both sides of the cutting seam are rough. This is attributed to the fact that the molten substances produced by wood combustion and vaporization in the laser action area are irregularly attached to both sides of the cutting seam or accumulated at the bottom of the cutting seam, so the processing quality is poor. It can be observed from Fig. 13b that when inert gas-assisted laser cutting wood, the processing quality of slit surface is significantly improved as the residue and carbide adhesion caused by incomplete combustion reaction are reduced under the protection of gas jet, and the impact cooling effect of air flow will discharge some materials that cannot be effectively burned from the bottom of slit, which reduces the solidified layer formed by the residue on the wall of the cutting seam. Hence, the cutting seam is relatively smooth and flat, and the cutting seam is relatively straight along the vertical direction. As seen in Fig. 13c, under the optimal test parameters, the cherry wood cutting seam surface is relatively smooth and there is almost no residue in the pores, which is due to the combination of various parameters of inert gas-assisted laser processing more reasonable and realization their positive significance. Under the synergistic action of laser and inert gas, the gas jet protects the cutting surface, reduced the damage of combustion exothermic reaction to the inner wall of cells through the flame retardant effect of air flow, and employes the cooling and scouring effect of air flow to take away the particle residue after gasification. Therefore, the quality of slit surface has been improved.

Conclusion

Utilizing helium-assisted laser processing and cutting wood technology can process high-quality cutting joints under the same energy consumption, save raw materials to a certain extent, and promote the improvement of forest coverage and environmental protection. After theoretical modeling and a series of experimental verification, the conclusions are listed as follows:

(1) Using helium-assisted laser processing, the helium ejected from the nozzle affects the combustion effect caused by the heat of high-temperature laser on wood, which reduces the carbonized layer of the processed slit, and then obtains better processing quality.
(2) Helium-assisted laser processing, the gas flow velocity of helium ejected from the injection port is 10 m/s. Helium not only affects the concentration of combustion-supporting gas, but also has a certain purging effect, which can eliminate the carbonized particles and residues of the processed slit, and improve the processing quality of the slit simultaneously.
(3) By comparing the traditional laser processing and inert gas-assisted laser processing wood cutting under the same process parameters, the inert gas-assisted laser processing has smaller slit width, surface roughness and smoother surface than the traditional laser processing. The cutting seam width and surface roughness of wood in the along-grain cutting mode are less than those in the cross-grain cutting mode.
(4) The response surface method is innovatively employed to establish the mathematical model with the slit width, slit depth and surface roughness as the evaluation criteria, to analyze the interaction of laser power, cutting speed and inert gas pressure on the response factors. Comparing the error between the predicted value of the quadratic mathematical model and the experimental measured value, the optimized the combination of process parameters could be acquired. When the laser power is 40 W, the cutting speed is 25.99 mm/s and the gas pressure is 0.15 MPa, the minimum surface roughness is 1.71 μm.
(5) When helium assisted laser cutting wood, the cutting seam quality and micromorphology are dramatically enhanced. On observing the micromorphology of the cutting seam by scanning electron microscope, it can be illumined that the cutting seam surface and around the pores of inert gas-assisted laser processing wood are relatively clear, almost no residues, which makes the inner wall complete and the surface smooth.

Abbreviation

RSM: Response surface methodology.

Acknowledgements

The authors thank many teachers of the school of mechanical and electrical engineering of Northeast Forestry University for their guidance and the laboratory of the school of mechanical and electrical engineering for their support.

Author contributions

CY is the project leader and responsible for the manuscript review. XT established the model, analyzed the data and drafted the manuscript. BX designed the experiment and put forward many modification suggestions for the manuscript. QL carried out specific experimental operation and data acquisition. JZ participated in electron microscope analysis and sample collection of processed wood. JL is one of the project leaders. WY is responsible for manuscript review and the corresponding author. All authors read and approved the final manuscript.

Funding

The work of this paper is jointly funded by the natural science foundation of Heilongjiang Province (ZD2021E001) and the special fund for basic scientific

research business expenses of Central Universities of the Ministry of education of China (2572019CP18).

Availability of data and materials
Most data analyzed during this study are included in this published article. The supplementary information is available from the corresponding author on reasonable request.

Declaration

Competing interests
The authors declare that they have no competing interests.

Author details
[1]Northeast Forestry University, 26 Hexing Rd, Harbin 150040, China. [2]Chinese Academy of Forestry, 1 DXF of Xiangshan Rd, Beijing 100091, China.

Received: 15 October 2021 Accepted: 13 July 2022
Published online: 27 August 2022

References

1. Xiang SL, Li CS (2010) Progress in wood processing and application technology. Science Press, Beijing
2. Wang BY (1994) Application of laser cutting in wood processing. China forestry science and technology 01:25–27
3. Zhang SH (2005) Research on laser cutting technology. D Sc Tech dissertation, Xi'an University of Technology.
4. Olakanmi EO, Cochrane RF, Dalgarno KW (2015) A review on selective laser sintering/melting (SLS/SLM) of aluminium alloy powders: Processing, microstructure, and properties. Prog Mater Sci 74:401–477
5. Naderi N, Legacey S, Chin SL (1999) Preliminary investigations of ultrafast intense laser wood processing. For Prod J 49(6):72–76
6. Kalyanasundaram D, Shehata G, Neumannc C, Shrotriya P, Molian P (2008) Design and validation of a hybrid laser/water-jet machining system for brittle materials. J Laser Appl 20(2):127
7. Lee M (2015) Recent Trends of the Material Processing Technology with Laser-ICALEO 2014 Review. J Weld Join 33(4):7–16
8. Lu Y, Ding Y, Wang ML (2021) An environmentally friendly laser cleaning method to remove oceanic micro-biofoulings from AH36 steel substrate and corrosion protection. J Clean Prod 314:127961
9. Xu SL (2018) Research and application of laser cutting equipment for complex curved surface. D Sc Tech dissertation, Shenyang University of Technology.
10. Lu Y, Yang LJ, Wang ML, Wang Y (2020) Improved thermal stress model and its application in ultraviolet nanosecond laser cleaning of paint. Appl Opt 59(25):7652–7659
11. Yang CM, Jiang T, Liu JQ, Ma Y, Miao Q (2020) Water admittance nanosecond laser ablation mechanism and processing experiment of Korean pine. Scientia Silvae Sinicae 56(08):204–211
12. Jiang XB, Hu H, Liu JQ, Zhu XL, Ma Y, Yang CM (2018) Discussion on the Processing of Wood by Nanosecond Water Guide Laser. Scientia Silvae Sinicae 54(01):121–127
13. Yang CM, Jiang T, Ma Y, Liu JQ (2019) Design and experimental study on water-jet assisted nanosecond laser equipment for wood. China forest products industry, 46(05):12–16+53.
14. American Meteorological Society (1935) Bulletin of The American Meteorological Society. 16(2): 31–33.
15. Siegman AE (1993) Defining, measuring, and optimizing laser beam quality. SPIE 1224:2–13
16. Li XC, Wang ZW (2016) Study on transient heat transfer process of one-dimensional thermoelectric module. Solar Newspaper 37(07):1826–1831
17. ISO 21920–2 (2021) Geometrical product specifications (GPS)—Surface texture: profile — Part 2: terms, definitions and surface texture parameters. International Organization for Standardization, Geneva

Publisher's Note